

## Combining Acid–Base, Redox and Substrate Binding Functionalities to Give a Complete Model for the [FeFe]-Hydrogenase

James M. Camara and Thomas B. Rauchfuss\*

School of Chemical Sciences, University of Illinois, Urbana, IL 61801

I. Supplementary Methods

II. Supplementary Tables

### Supplementary Table 1: Magnetic Susceptibility Data

III. Supplementary Figures

**Supplementary Figure 1:** Cyclic voltammogram of  $Fc^*P$  in  $CH_2Cl_2$  referenced to  $Fc/Fc^+$ .

**Supplementary Figure 2:** Cyclic voltammogram of **1** in  $CH_2Cl_2$  referenced to  $Fc/Fc^+$ .

**Supplementary Figure 3:** Experimental and simulated X-band EPR spectra of  $[1]^+$  at 110 K in a 50/50  $CH_2Cl_2$ /toluene glass.

**Supplementary Figure 4:** X-band EPR spectrum of  $[1]^{2+}$  at 4.5 K and 10 dB power in a 50/50  $CH_2Cl_2$ /toluene glass.

**Supplementary Figure 5:** X-band EPR spectrum of  $[1]^{2+}$  at 4.5 K and 30 dB power in a 50/50  $CH_2Cl_2$ /toluene glass.

**Supplementary Figure 6:** Plot of  $1/\chi_M$  vs temperature for  $[1]^+$ .

**Supplementary Figure 7:** Plot of  $1/\chi_M$  vs temperature for  $[1]^{2+}$ .

**Supplementary Figure 8:** NMR stack plot of reaction of  $[1]^{2+}$  and  $P(o\text{-tol})_3$  with  $H_2$  and  $D_2$ .

**Supplementary Figure 9:** Kinetic plot for the reaction of  $[1]^{2+}$  with  $H_2$  in the presence of  $P(o\text{-tol})_3$  fit to a first order exponential. *Inset:* Linearized kinetic plot illustrating first-order kinetics.

**Supplementary Figure 10:**  $^{31}P$  NMR stack plot showing catalytic oxidation of  $H_2$  by  $[1]^{2+}$  in the presence of excess  $FcBAr^F_4$  and excess base.

## I. Supplementary Methods

All procedures were carried out using standard Schlenk Techniques. All solvents were dried and degassed using by passage through activated alumina and sparging with argon respectively. IR spectra were recorded on a Perkin Elmer Spectrum 100. NMR spectra were recorded on a Varian Unity 500Mhz NMR Spectrometer. X-band EPR spectra were collected on a Varian E-122 spectrometer equipped with an E-257 variable-temperature accessory. Magnetic fields were calibrated using a Varian NMR Gauss meter. The microwave frequency was measured with an EIP frequency meter. EPR simulations were carried out using the program SIMPOW6.

**Generation of  $[\text{Fe}_2(\text{adt}^{\text{Bn}})(\text{CO})_3(\text{dppv})(\text{Me}_9\text{FcCH}_2\text{PEt}_2)][\text{BAr}^{\text{F}}_4]_2$ , ( $[\mathbf{1}]^{2+}$ ).** *Via titration of  $\text{FcBAr}^{\text{F}}_4$  into  $\mathbf{1}$ .* A solution of  $\mathbf{1}$  (15 mg, 12.5  $\mu\text{mol}$ , in 5 mL dichloromethane) was titrated with a solution of  $\text{FcBAr}^{\text{F}}_4$  (26.15 mg, 25  $\mu\text{mol}$ , in 2 mL dichloromethane) in 0.5 mL aliquots. Upon addition of the oxidant, the solution turned from brown-orange to purple. The reaction was monitored by IR after each 0.5 mL addition of oxidant. After 1.0 equiv of oxidant was added, all starting material was consumed and the IR spectrum ( $\nu_{\text{CO}} = 2012$  (s), 1961 (s), 1859 (w)  $\text{cm}^{-1}$ ) was assigned to  $[\mathbf{1}]^+$ . After addition of 2.0 equiv of oxidant, the IR spectrum changed ( $\nu_{\text{CO}} = 2015$  (s), 1965 (s), 1849 (w)  $\text{cm}^{-1}$ ) and the resulting species was assigned to  $[\mathbf{1}]^{2+}$ . An isosbestic point at 1969  $\text{cm}^{-1}$  upon conversion of  $[\mathbf{1}]^+$  to  $[\mathbf{1}]^{2+}$  was observed (Figure 4).

**EPR measurements of  $[\mathbf{1}]^+$  and  $[\mathbf{1}]^{2+}$ :**  $[\mathbf{1}]^+$ . A solution of  $\mathbf{1}$  (5 mg, 4.1  $\mu\text{mol}$ ) in 2 mL toluene and a solution of  $\text{FcBAr}^{\text{F}}_4$  (4.4 mg, 4.1  $\mu\text{mol}$ ) in 2 mL of  $\text{CH}_2\text{Cl}_2$  were mixed under inert atmosphere. 300  $\mu\text{L}$  of the resulting purple solution was transferred to an EPR tube with J. Young valve. The solution was frozen in liquid nitrogen to form a glass. X-band EPR was collected at 110 K and is shown in Supplementary Figure 3. Simulation shows predominantly rhombic (xy) splitting and an additional small (5 to 20 MHz) third  $^{31}\text{P}$  splitting from  $\text{Fc}^*\text{P}$ .

$[\mathbf{1}]^{2+}$ . A solution of  $\mathbf{1}$  (5 mg, 4.1  $\mu\text{mol}$ ) in 2 mL toluene and a solution of  $\text{FcBAr}^{\text{F}}_4$  (8.8 mg, 8.2  $\mu\text{mol}$ ) in 2 mL of  $\text{CH}_2\text{Cl}_2$  were mixed under inert atmosphere. 300  $\mu\text{L}$  of the resulting purple solution was transferred to an EPR tube with J. Young valve. The solution was frozen in liquid nitrogen to form a glass. X-band EPR was collected at 110 K and showed a small amount of  $[\mathbf{1}]^+$  and no signal for  $[\mathbf{1}]^+$ . Upon cooling to 4.5 K an additional broad signal appears at  $g \approx 1.66$  (Supplementary Figure 4). Upon increasing the power from 10 dB to 30dB, the residual signal for  $[\mathbf{1}]^+$  saturates, but the signal for  $[\mathbf{1}]^{2+}$  does not (Supplementary Figure 5).

**Magnetic Susceptibility of  $[\mathbf{1}]^+$ :** Magnetic susceptibility measurements were carried out using Evans' Method.<sup>1-3</sup> A melting point capillary was sealed with pure  $\text{CD}_2\text{Cl}_2$ . A J. Young tube was charged with a solution of  $\mathbf{1}$  (7 mg, 5.8  $\mu\text{mol}$ ) and  $\text{FcBAr}^{\text{F}}_4$  (6.1 mg, 5.8  $\mu\text{mol}$ ) in 0.7 mL  $\text{CD}_2\text{Cl}_2$ . The capillary was inserted into the tube, and the solution analyzed by  $^1\text{H}$  NMR at various temperatures. The temperature of the NMR probe was calibrated using a 100% methanol standard. The difference in the chemical shift of the residual solvent resonance in the capillary and the residual solvent resonance in the solution was measured from the center of the corresponding 1:1:1 triplets. The following formula yields the magnetic susceptibility where  $\Delta\nu$

is the peak separation in Hz,  $\nu_1$  is the spectrometer frequency in Hz, and  $c$  is the solute concentration in mol/L:

$$\chi_M = (477) \frac{\Delta\nu}{2\nu_1 c}$$

The data are in Table 1. The slope of a plot of  $1/\chi_M$  vs temperature (Supplementary Figure 6) yields the Curie constant,  $C$ , from which the number of unpaired electrons ( $n$ ) may be calculated using the following formula:

$$C = \frac{1}{8} n(n + 2)$$

The magnetic moment may also be calculated from the following:

$$\mu_{\text{eff}} = \sqrt{8\chi_M T}$$

The magnetic moments calculated for  $[1]^+$  and  $[1]^{2+}$  match those expected for species with 1 and 2 unpaired electrons (1.73 BM and 2.83 BM respectively).

**Magnetic Susceptibility of  $[2]^+$ :** Magnetic susceptibility measurements were carried out as above using a solution of **1** (7 mg, 5.8  $\mu\text{mol}$ ) and  $\text{FcBAR}^{\text{F}_4}$  (12.2 mg, 11.6  $\mu\text{mol}$ ) in 0.7 mL  $\text{CD}_2\text{Cl}_2$ . A plot of  $1/\chi_M$  vs temperature is in Supplementary Figure 7.

**Reaction of  $[1]^{2+}$  with  $\text{D}_2$ :** A J. Young tube was charged with a solution of **1** (4.2 mg, 3.5  $\mu\text{mol}$ ),  $\text{P}(o\text{-tol})_3$  (1 mg, 3.5  $\mu\text{mol}$ ), and  $\text{FcBAR}^{\text{F}_4}$  (7.3 mg, 7.0  $\mu\text{mol}$ ) in 0.7 mL  $\text{CH}_2\text{Cl}_2$ . The tube was then evacuated, pressurized with 14.5 psig  $\text{D}_2$ , shaken, and allowed to react at 0 °C overnight.  $^2\text{H}$  NMR (97 MHz,  $\text{CD}_2\text{Cl}_2$ )  $\delta$  = 8.4 ppm (d,  $J_{\text{P-D}}$  = 74 Hz, 1D), -15.4 (bs, 1D). The spectrum is in Supplementary Figure 8.

**Rate of  $\text{H}_2$  oxidation by  $[1]^{2+}$ :** A J. Young tube was charged with a solution of **1** (4.2 mg, 3.5  $\mu\text{mol}$ ),  $\text{P}(o\text{-tol})_3$  (1 mg, 3.5  $\mu\text{mol}$ ),  $\text{FcBAR}^{\text{F}_4}$  (7.3 mg, 7.0  $\mu\text{mol}$ ) and  $\text{HFe}_2(\text{adt}^{\text{Bn}})(\text{PMe}_3)_2(\text{CO})_4[\text{PF}_6]$  (2.1 mg, 4.0  $\mu\text{mol}$ ) as internal standard in 0.7 mL  $\text{CD}_2\text{Cl}_2$ . The tube was then evacuated, pressurized with 14.5 psig  $\text{H}_2$ , shaken, and cooled to 0 °C. The reaction was monitored by appearance of the product hydride peak at -15.33 ppm in the  $^1\text{H}$  NMR. Under the reaction conditions,  $\text{H}_2$  dissolved more quickly than it was consumed, and was present in large excess. The appearance of product hydride  $[\text{1H}]^+$  was strictly first order with observed pseudo-first order rate constant  $k_{\text{obs}} = 8.3(4) \times 10^{-5} \text{ s}^{-1}$  (Supplementary Figure 9).

**Catalytic oxidation of  $\text{H}_2$  using  $[1]^{2+}$ :** A J. Young tube was charged with a solution of **1** (4.2 mg, 3.5  $\mu\text{mol}$ ),  $\text{P}(o\text{-tol})_3$  (6.4 mg, 21  $\mu\text{mol}$ ),  $\text{FcBAR}^{\text{F}_4}$  (22 mg, 21  $\mu\text{mol}$ ) and  $\text{HFe}_2(\text{adt}^{\text{Bn}})(\text{PMe}_3)_2(\text{CO})_4[\text{PF}_6]$  (2.1 mg, 4.0  $\mu\text{mol}$ ) as internal standard in 0.7 mL  $\text{CD}_2\text{Cl}_2$ . The tube was then evacuated, and pressurized with 14.5 psig  $\text{H}_2$ . The reaction was monitored by observing the disappearance of  $\text{P}(o\text{-tol})_3$  and appearance of  $[\text{HP}(o\text{-tol})_3][\text{BAR}^{\text{F}_4}]$  in the  $^{31}\text{P}$  NMR spectrum ( $\delta$  = -12.3(s) and -28.9(s) respectively). During the course of the reaction the solution changed from purple to orange. After 5h, complete conversion of  $\text{P}(o\text{-tol})_3$  to  $[\text{HP}(o\text{-tol})_3][\text{BAR}^{\text{F}_4}]$  was observed (Supplementary Figure 10).

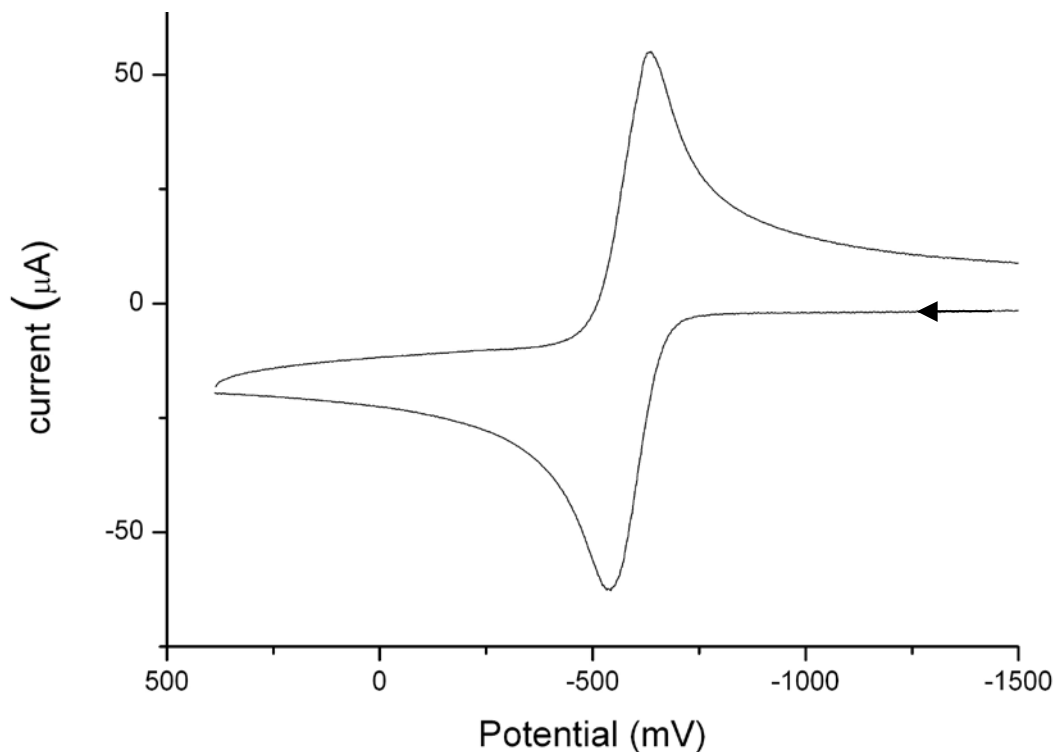
## II. Tables

**Table 1:** Magnetic Susceptibility Data

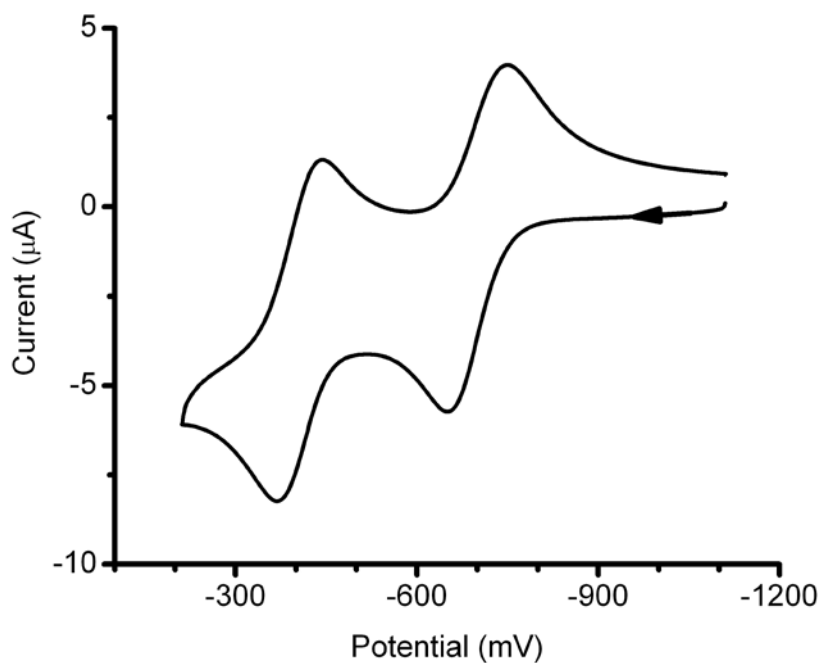
Temp	<b>[1]<sup>+</sup></b>				<b>[2]<sup>+</sup></b>			
	$\Delta\delta$ (Hz)	$\chi_m$	# electrons	$\mu_{\text{eff}}$	$\Delta\delta$ (Hz)	$\chi_m$	# electrons	$\mu_{\text{eff}}$ (BM)
298.5	21.86	.00126	} 0.9(2)	1.8(1)	60.61	.00348	} 1.8(2)	2.9(1)
272.1	25.40	.00146			69.57	.00400		
255.0	26.60	.00153			74.07	.00423		

## III. Supplementary Figures

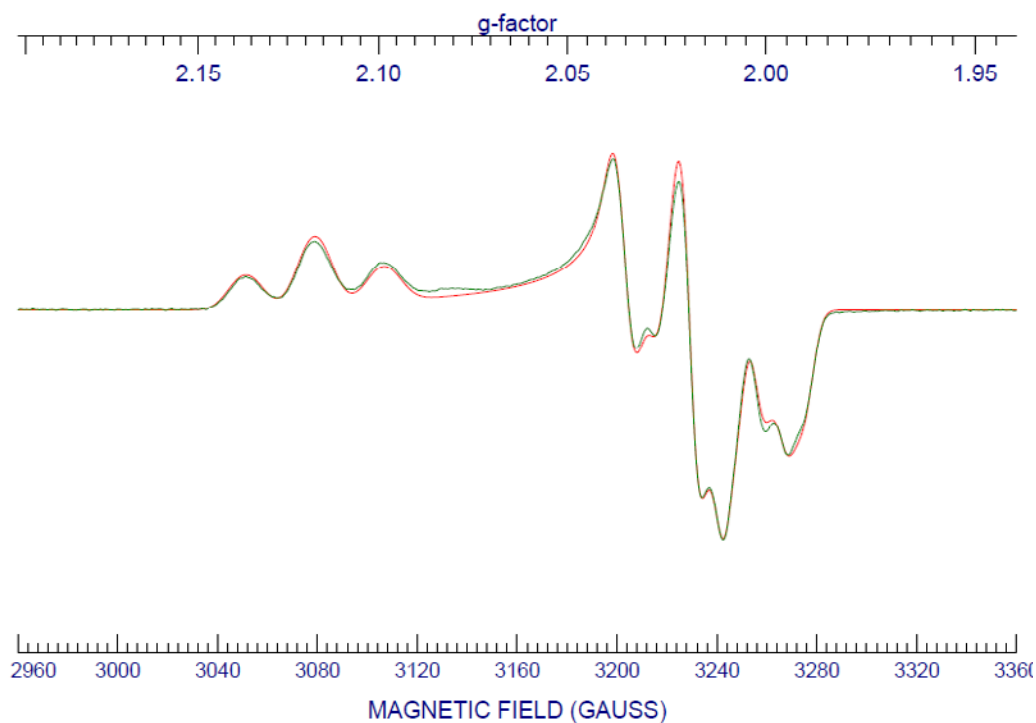
**Supplementary Figure 1.** Cyclic voltammogram of (Diethylphosphinomethyl)nonamethylferrocene (*Fc\*P*) in  $\text{CH}_2\text{Cl}_2$  referenced to  $\text{Fc}/\text{Fc}^+$ . [*Fc\*P*] = 1 mM, [TBA][ $\text{BAR}_4^{\text{F}}$ ] = 100 mM, scan rate = 300 mV/s, IR compensation at -950 mV,  $E_{1/2} = -591$  mV ( $I_{\text{pa}}/I_{\text{pc}} = 0.95$ )



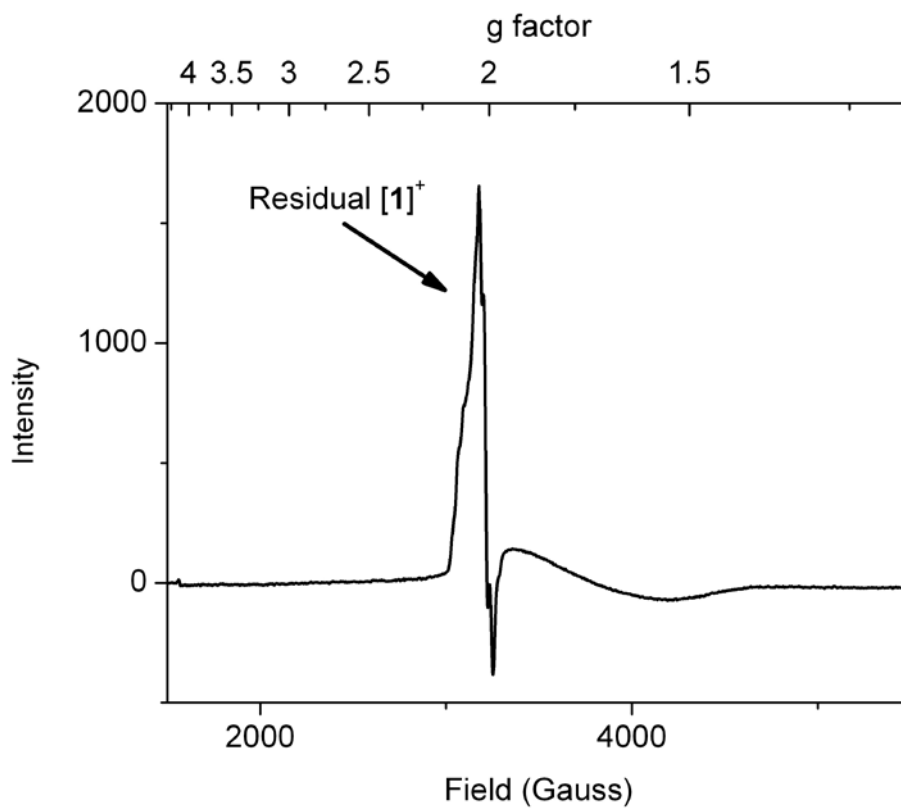
**Supplementary Figure 2:** Cyclic voltammogram of **1** in CH<sub>2</sub>Cl<sub>2</sub> referenced to Fc/Fc<sup>+</sup>. [**1**] = 1 mM, [TBA][BAR<sup>F</sup><sub>4</sub>] = 100 mM, scan rate = 100 mV/s, IR compensation at -950 mV, E<sub>1/2</sub> = -393 mV (I<sub>pa</sub>/I<sub>pc</sub> = 0.90), E<sub>1/2</sub> = -700 mV (I<sub>pa</sub>/I<sub>pc</sub> = 0.85).



**Supplementary Figure 3:** Experimental (red) and Simulated (green) X-band EPR spectrum of  $[1]^+$  at 110 K in a 50/50  $\text{CH}_2\text{Cl}_2$ /toluene glass.  $g_z = 2.1174$  with  $A_z(^{31}\text{P}) = 79.9$  MHz,  $g_x \approx g_y = 2.0190$  with  $A_x(^{31}\text{P}) \approx A_y(^{31}\text{P}) = 67.7$  MHz.

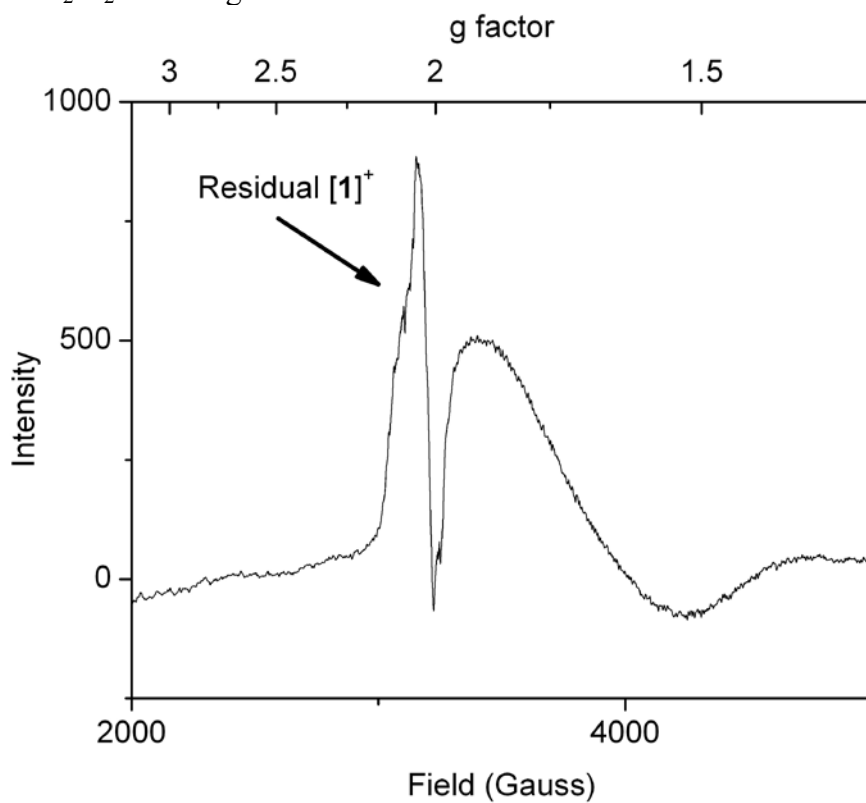


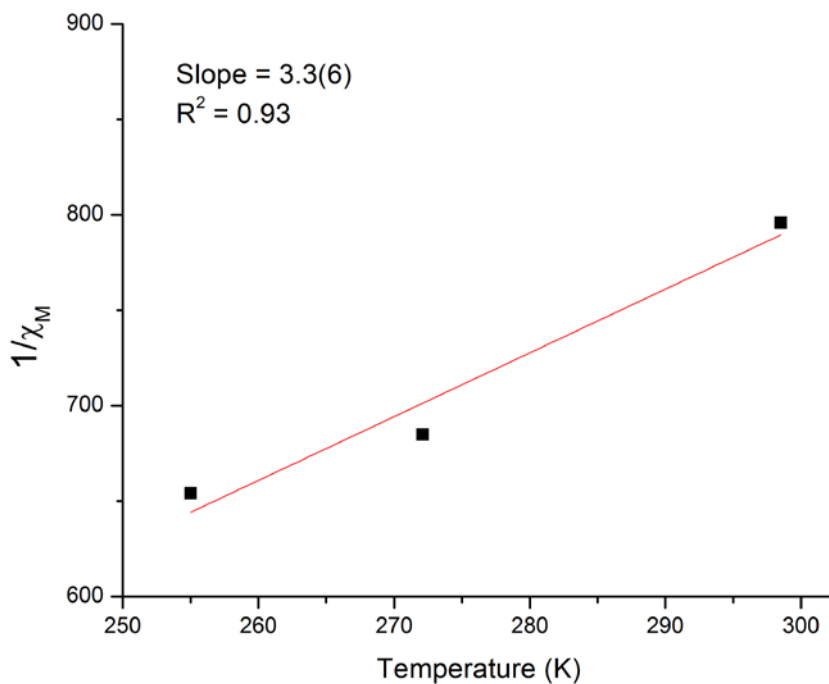
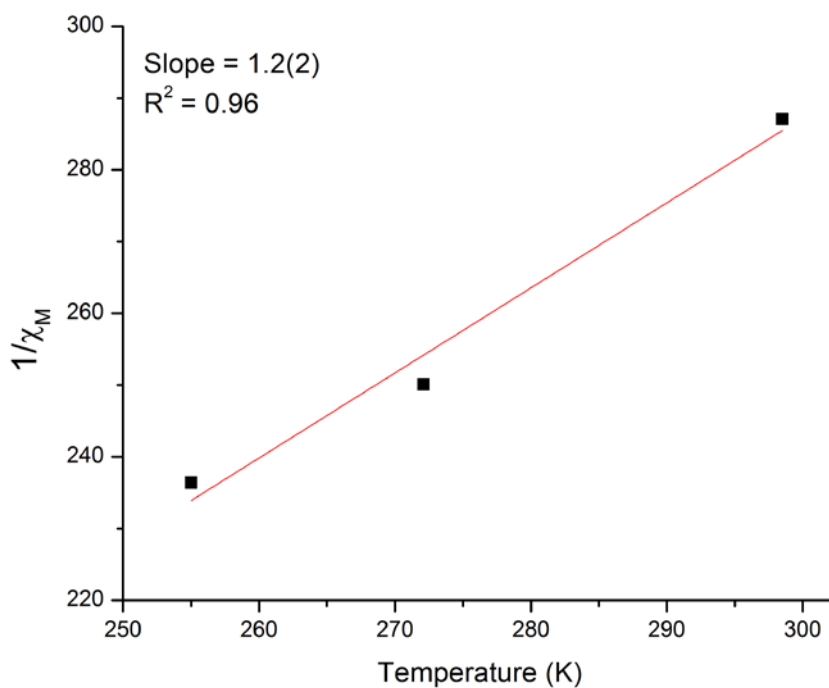
**Supplementary Figure 4:** X-band EPR spectrum of  $[1]^{2+}$  at 4.5 K and 10 dB power in a 50/50  $\text{CH}_2\text{Cl}_2$ /toluene glass.



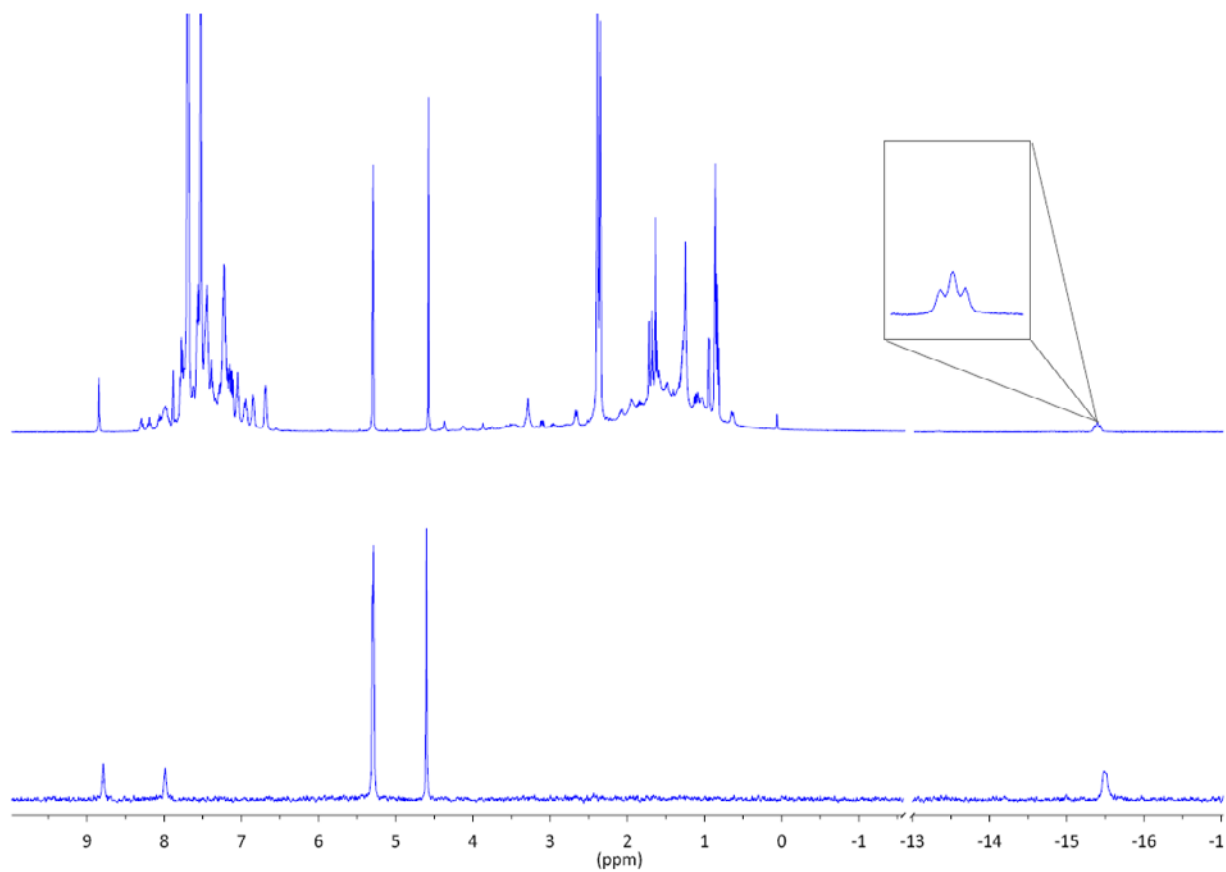


**Supplementary Figure 5:** X-band EPR spectrum of  $[1]^{2+}$  at 4.5 K and 30 dB power in a 50/50  $\text{CH}_2\text{Cl}_2$ /toluene glass.

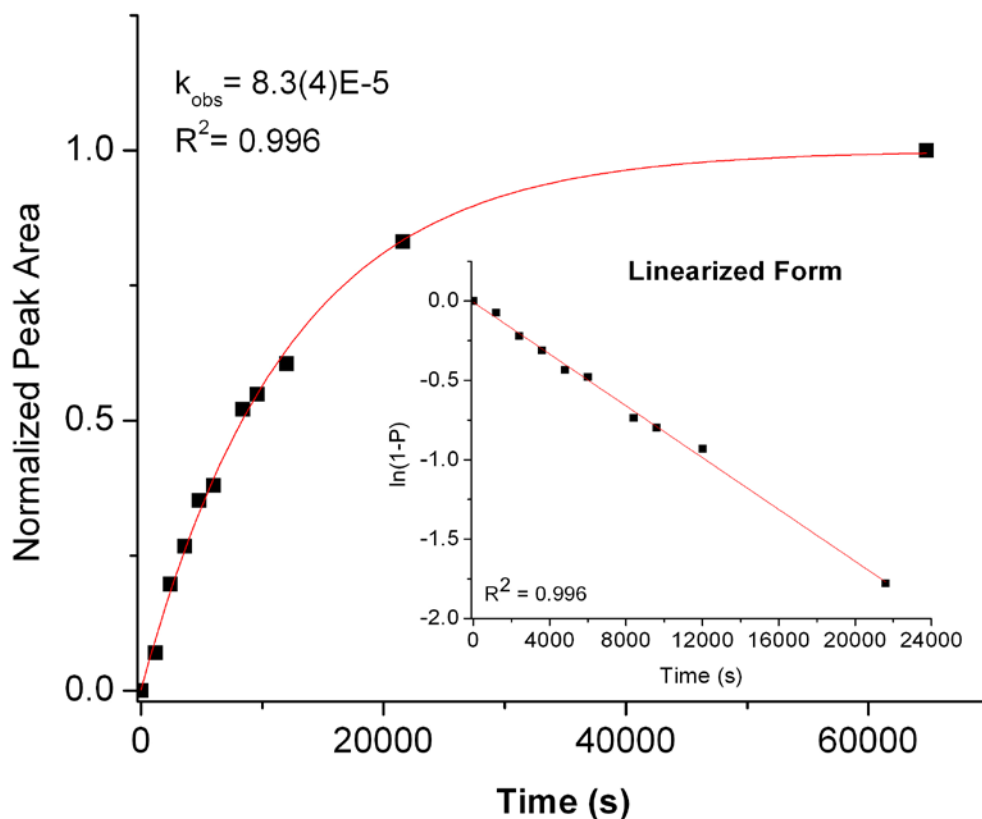


**Supplementary Figure 6:** Plot of  $1/\chi_M$  vs temperature for  $[1]^+$ .**Supplementary Figure 7:** Plot of  $1/\chi_M$  vs temperature for  $[1]^{2+}$ .

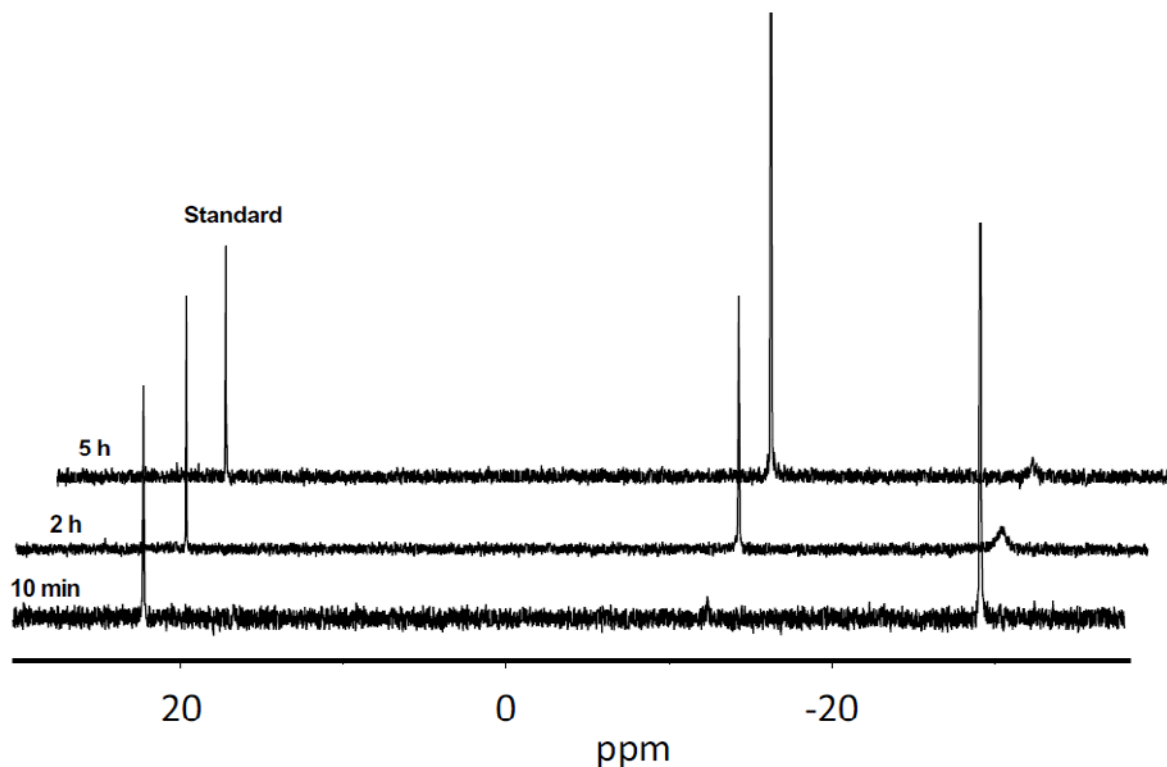
**Supplementary Figure 8:** NMR stack plot of reaction of  $[1]^{2+}$  and  $P(o\text{-tol})_3$  with  $H_2$  and  $D_2$ . *Top:*  $^1H$  NMR (500 MHz,  $CD_2Cl_2$ ) of  $H_2$  activation reaction. *Bottom:*  $^2H$  NMR (97 MHz,  $CD_2Cl_2$ ) of  $D_2$  activation reaction. The  $^2H$  NMR shows  $^2H$  incorporation into the product hydride and phosphonium.



**Supplementary Figure 9:** Kinetic plot for the reaction of  $[1]^{2+}$  with  $H_2$  in the presence of  $P(o\text{-tol})_3$  fit to a first order exponential. *Inset:* Linearized kinetic plot illustrating first-order kinetics.



**Supplementary Figure 10:**  $^{31}\text{P}$  NMR stack plot showing catalytic oxidation of  $\text{H}_2$  by  $[\mathbf{1}]^{2+}$  in the presence of excess  $\text{FcBAR}^{\text{F}}_4$  and excess base.  $\delta = -12.3$  (s,  $[\text{HP}(o\text{-tol})_3]^+$ ),  $-28.9$  (s,  $\text{P}(o\text{-tol})_3$ ).



- 1 Evans, D. F. The determination of the paramagnetic susceptibility of substances in solution by nuclear magnetic resonance. *J. Chem. Soc.* 2003-2005 (1959).
- 2 Sur, S. K. Measurement of magnetic susceptibility and magnetic moment of paramagnetic molecules in solution by high-field fourier transform nmr spectroscopy. *J. Mag. Reson.* **82**, 169-173 (1989).
- 3 Girolami, G. S., Rauchfuss, T. B. & Angelici, R. J. *Synthesis and technique in inorganic chemistry*. (University Science Books, 1999).